

# NACA

## RESEARCH MEMORANDUM

LONGITUDINAL STABILITY AND DRAG CHARACTERISTICS OF A  
FIN-STABILIZED BODY OF REVOLUTION WITH A  
FINENESS RATIO OF 12 AS MEASURED  
BY THE FREE-FALL METHOD

By Max C. Kurbjun

Langley Aeronautical Laboratory  
Langley Field, Va.

CLASSIFIED DOCUMENT

to an unauthorized person is prohibited by law.

### NATIONAL ADVISORY COMMITTEE FOR AERONAUTICS

WASHINGTON

June 24, 1954



## NATIONAL ADVISORY COMMITTEE FOR AERONAUTICS

## RESEARCH MEMORANDUM

LONGITUDINAL STABILITY AND DRAG CHARACTERISTICS OF A  
FIN-STABILIZED BODY OF REVOLUTION WITH A  
FINENESS RATIO OF 12 AS MEASURED  
BY THE FREE-FALL METHOD

By Max C. Kurbjun

## SUMMARY

Measurements of the longitudinal stability and drag characteristics of a fin-stabilized body of revolution with a fineness ratio of 12 at low angles of attack have been made through the transonic speed range by the free-fall method.

The results showed that the aerodynamic center moved rearward from 55 percent body length ahead of the nose at a Mach number of 0.87 and a body normal-force coefficient of 0.11 to 15 percent ahead of the nose at a Mach number of 1.26 and a body normal-force coefficient of 0.24. By the theory of NACA RM A9I26, approximately 60 percent of this shift in aerodynamic center would be expected to accompany the increase in body normal-force coefficient. The rest is assumed to be attributable to the change in Mach number. The same trend was indicated in the investigation of a similar model reported in NACA RM L52D21a.

The longitudinal-force coefficients of the present configuration at subsonic speeds agree favorably with the zero-lift drag coefficients of a similar configuration reported in NACA RM L9J27. At supersonic speeds, however, the longitudinal-force coefficients were 20 percent less than the zero-lift drag of NACA RM L9J27.

## INTRODUCTION

Much effort has been expended in the past to obtain satisfactory stability and to reduce the drag of high-speed aircraft. The present investigation was proposed in order to determine the contribution to the

stability and drag that the body produces at an angle of attack. The free-fall method was used to obtain this information through the transonic speed range in free air and at high Reynolds numbers for comparison with investigations using other methods and theoretical analyses.

The configuration investigated consisted of a fineness-ratio-12 body of revolution with cruciform tail surfaces attached to the body by means of a tail boom. The horizontal tail surfaces were installed with  $5^\circ$  angle of incidence to the body center line which theoretically would trim the model at  $7^\circ$  angle of attack.

The Mach number in the present investigation ranged from subsonic to 1.26, and the body normal-force coefficient ranged from 0.11 to 0.24. The results of the present investigation are compared with the theoretical variation of lift and stability from reference 1 and with the results of lift and stability measurements made in wind-tunnel investigations reported in reference 2. Drag comparisons are made with the zero-lift drag of a similar model investigated in reference 3.

#### SYMBOLS

a.c.	body aerodynamic-center location, percent $\bar{c}$
$a_C$	longitudinal acceleration, g units
$a_N$	normal acceleration, g units
$\bar{c}$	length of body, ft
$C_C$	longitudinal-force coefficient, $W a_C / qS$
$C_D$	drag coefficient, $D / qS$
$C_{M_B}$	body moment coefficient, $M_B / qS\bar{c}$
$dC_M / d\alpha$	static longitudinal stability (body plus tail)
$C_{N_B}$	body normal-force coefficient, $\frac{W a_N - M_B / t}{qS}$
D	drag of complete configuration, lb
f	frequency of oscillation in pitch for complete model, cps

CONFIDENTIAL

$I_y$	moment of inertia about lateral axis (complete model), $\text{ft}^4$
$M$	Mach number
$M_B$	measured body moment about center of gravity, $\text{ft-lb}$
$M_B'$	corrected body moment about body midpoint, $\text{ft-lb}$
$p$	static pressure, $\text{lb/ft}^2$
$q$	dynamic pressure, $\frac{\gamma}{2} \rho M^2$ , $\text{lb/ft}^2$
$S$	body frontal area, $\text{ft}^2$
$t$	tail length (center of gravity to 40 percent chord of horizontal stabilizer), $\text{ft}$
$W$	model weight, $\text{lb}$
$\gamma$	ratio of specific heats

#### APPARATUS AND METHOD

##### Model Configuration

The model consisted of a fineness-ratio-12 body, similar to those used in a previous investigation in the free-fall program and reported in reference 3, and a cruciform unswept tail surface. A photograph of the model and a drawing giving pertinent dimensions are presented in figures 1 and 2, respectively. Coordinates of the body are given in table I.

The cruciform tail surfaces were made of solid steel with a constant chord section. The vertical and horizontal surfaces were mounted on a 2-inch boom with  $0^\circ$  and  $5^\circ$  angle of incidence, respectively, to the boom. A photograph of the tail boom and stabilizing surfaces is shown in figure 3.

The center of gravity of the model was located 12.1 inches ahead of the body midpoint, the total weight was 672.5 pounds, and the moment of inertia about a lateral axis through the center of gravity was 130 slug-feet<sup>2</sup>.

### Instrumentation and Measurements

In addition to the measurement of the flight path of the model, which was obtained from the radar and phototheodolite equipment, the following quantities were telemetered from the model: normal (perpendicular to the longitudinal body axis and perpendicular to the lateral axis of the offset tail), transverse, and longitudinal accelerations (accelerometers at the center of gravity), and rate of roll and body moment about the center of gravity. The accelerations were measured with instruments similar to those described in reference 3 and the rate of roll was measured by a standard NACA roll turnmeter adapted for telemeter use. Body moment was measured by a double-bar cantilever balance mounted between the rear of the body and the tail boom. The deflection of the balance under a load was relayed to the telemetering equipment by an inductance-type pickup coil. A drawing of the balance and pickup coil is shown in figure 2. This type of balance has the advantage that, by mounting the cantilever bars at an angle such that the apex of the angle is located at the center of gravity, as shown in figure 2, the entire tail assembly will rotate under load about the center of gravity; thus, the displacement of the balance at the pickup will be a true measure of the body moment about the center of gravity. For the small displacement necessary at the pickup, in order to measure the body moment, the angular displacement of the tail surfaces from the longitudinal axis will be relatively small.

An attempt was also made to measure the angle of attack of the model by means of an angle-of-attack indicator mounted on a nose boom (figs. 1 and 2). These measurements failed during the test because of apparent damage to the nose-boom installation before or during the release of the model.

Atmospheric surveys were obtained from synchronized records of atmospheric pressure, temperature, and radar-obtained geometric altitudes taken during the ascent and descent of the drop aircraft before and after the drop of the model. The direction and velocity of the horizontal component of the wind was determined from radar and phototheodolite records obtained from the ascent of a free balloon after the free fall of the model.

Mach number was obtained during the fall from the radar-velocity data previously described and the use of the atmospheric wind and temperature data. The estimated uncertainty in the values of Mach number is less than  $\pm 0.01$ ; this uncertainty has been verified in previous investigations.

### Reduction of Data

The coefficients presented in this paper were determined from the values of model weight  $W$ , body frontal area  $S$ , acceleration  $a$  (in

g units), and dynamic pressure  $q$ . For the body normal-force coefficient  $C_{NB}$ , the following relationship was applied:

$$C_{NB} = \frac{W a_N - M_B/t}{S q}$$

where  $M_B$  is the measured body moment about the center of gravity,  $t$  is the distance from the 40 percent chord of the horizontal stabilizer to the center of gravity of the model, and  $a_N$  is the normal acceleration of the model.

The longitudinal-force coefficient  $C_C$  was calculated using the relation

$$C_C = \frac{W a_C}{S q}$$

where  $a_C$  is the longitudinal acceleration of the model.

In order to compare the longitudinal-force coefficient with the zero-lift drag of a similar model previously investigated, a correction was applied to  $C_C$  for the incremental thrust along the body axis produced by the stabilizer.

The moment about the midpoint of the body was determined by the measured body moment about the center of gravity plus the product of the body lift and the distance from the center of gravity to the body midpoint. Also, a correction was applied to the body moment for the moment created by centrifugal forces due to the rotation of the body while at an angle of attack. The angle of attack was approximated by the theory of reference 1 from the body normal-force coefficient; the rate of roll at Mach numbers above 1.15 was estimated by the extrapolation of the rate-of-roll measurement beyond the limits of the instrument. The moment correction was approximately 10 percent of the corrected body moment at  $M = 0.9$  and increased to 15 percent at  $M = 1.15$  and to 20 percent at  $M = 1.25$ . The correction in the lower range of Mach number is subject to errors in proportion to the sine of the error in determining the angle of attack; however, a difference as large as  $3^\circ$  between the theory and the investigation would introduce an error of less than 3 percent in the corrected moment. The corrections above  $M = 1.15$  are subject to greater errors because of the extrapolated rate of roll, the centrifugal forces being proportional to the square of the rate of roll.

By using the body moment about the midpoint of the body corrected for roll  $M_B'$  the moment coefficient was obtained as follows:

$$C_{MB} = \frac{M_B'}{S\bar{c}q}$$

The static-longitudinal-stability parameter  $dC_M/d\alpha$  for the body and tail combination under rolling conditions was determined from the following relation:

$$\frac{dC_M}{d\alpha} = \frac{(2\pi f)^2 I_Y}{qS\bar{c}}$$

where  $f$  is the frequency of the oscillation of the model in either pitch or yaw while rolling and  $I_Y$  is the moment of inertia about a lateral axis through the model's center of gravity. Values of  $dC_M/d\alpha$  were determined for the nonrolling conditions from the same relation but by applying corrections to the values of the frequency of the oscillation in pitch while rolling by the method presented in reference 4.

## RESULTS AND DISCUSSION

### Basic Results

The basic measurements made during the free fall of the model are presented as a time history in figure 4. The body moment about the model center of gravity, normal acceleration, transverse acceleration, longitudinal acceleration, and rate of roll were determined directly from the telemeter records. The variation of Mach numbers and static pressure with time, as determined from the radar and atmospheric temperature pressure survey, is also presented in figure 4.

The first 25 seconds of drop records were unusable for test data because of oscillations in attitude developed at release. These oscillations did not begin to damp until a Mach number of 0.68 (25 seconds) was attained, and at  $M = 0.90$  (34 seconds), the oscillations were completely damped. Data from 48 seconds ( $M = 1.26$ ) to impact were unusable because of uncontrolled gyrations of the model which will be discussed subsequently.

Body moment increased with Mach number. At  $M = 0.68$  (25 seconds), the oscillations were  $\pm 400$  foot-pounds with a mean of approximately 250 foot-pounds. This mean increased during the damped oscillation to

350 foot-pounds at  $M = 0.91$  (34 seconds) and the increase was then more rapid to 1,350 foot-pounds at  $M = 1.26$  (48 seconds).

The mean normal acceleration was approximately  $0.1g$  during the oscillations with  $\pm 0.15g$  at  $M = 0.68$  (25 seconds) becoming damped at  $M = 0.91$  (34 seconds). Normal acceleration increased during the remainder of the usable fall to  $0.7g$  at  $M = 1.26$  (48 seconds).

Longitudinal acceleration increased with Mach number from  $-0.025g$  with  $\pm 0.03g$  oscillation at  $M = 0.68$  (25 seconds) to  $0.05g$  at  $M = 0.91$  (34 seconds). A rapid increase occurred at  $M = 0.95$  (35 seconds) from  $0.075g$  to  $0.125g$  and then increased more gradually to  $0.34g$  at  $M = 1.26$  (48 seconds).

The variation of the transverse acceleration was  $\pm 0.15g$  about a mean of approximately  $-0.05g$  (left sideslip) at  $M = 0.68$  (25 seconds), damping to  $-0.02g$  at  $M = 0.91$  (34 seconds). A buildup of transverse acceleration began at  $M = 1.12$  (40 seconds) and became  $-0.4g$  at  $M = 1.26$  (48 seconds).

Rate of roll remained at approximately  $100^\circ$  per second from 25 to 35 seconds ( $M = 0.68$  to  $M = 0.94$ ) and increased rapidly to the instrument limit of  $180^\circ$  per second at 41 seconds ( $M = 1.15$ ). An extrapolation of the rate of roll used to correct the body-moment measurement is shown as the dashed line from 41 to 48 seconds.

#### Experimental Coefficients

The variation of body normal-force, total longitudinal-force, and body moment coefficients with Mach number is presented in figure 5. Also included is the zero-lift drag coefficient of the body and tail previously investigated (ref. 3) and the total longitudinal-force coefficient of the present investigation plus the thrust due to the tail surface. Coefficients were not presented below a Mach number of 0.85 because of the inaccuracies involved in determining the coefficients during the oscillating portion of the investigation.

The longitudinal-force coefficient increased abruptly from about 0.1 at  $M = 0.93$  to 0.25 at  $M = 0.98$ . As the Mach number increased, longitudinal-force coefficient decreased rapidly to 0.19 at  $M = 1.05$ , and more gradually to 0.18 at  $M = 1.26$ . The longitudinal thrust due to the lifting tail surface was approximately 0.01 subsonic and 0.015 supersonic. The zero lift drag of the model of reference 3 agreed with the longitudinal force at the subsonic speeds but was approximately 20 percent less at supersonic speeds. For a body of revolution at the low lift coefficients encountered, the theory of reference 1 predicts



that the longitudinal-force coefficient and zero-lift drag coefficient should be approximately the same.

Normal-force coefficient varied from 0.11 to 0.15 through the drag rise. From  $M = 1.05$  to  $M = 1.22$ ,  $C_{NB}$  remained approximately 0.15, increasing rapidly with Mach number to 0.24 at  $M = 1.25$ .

The body moment coefficient  $C_{MB}$  did not vary with Mach number or normal-force coefficient and remained at approximately 0.13 throughout the range of the investigation.

Presented in figure 6 is the aerodynamic-center position against normal-force coefficient variation for the present investigation. Included is the aerodynamic-center position determined by the theory of reference 1 and for the similar body of reference 2; the band shown for reference 2 covers Mach numbers from 0.89 to 1.13. In order to show the variation of Mach number for the present investigation during the shift in aerodynamic center shown by figure 6, a curve of body normal-force coefficient against Mach number is presented in figure 7.

The results show that the aerodynamic center moved rearward from 55 percent body length ahead of the nose at  $C_{NB} = 0.11$  and  $M = 0.87$  to 15 percent ahead of the nose at  $C_{NB} = 0.24$  and  $M = 1.26$ . The theory of reference 1 shows 60 percent of this shift in aerodynamic center to be due to the increase in  $C_{NB}$ . The theoretical increase in  $C_{NB}$  for this body is due primarily to viscous cross forces and is a nonlinear variation with increasing angle of attack. The balance of the shift in aerodynamic center is assumed attributable to the change in Mach number. The variation of aerodynamic-center position with  $C_{NB}$  for the model of reference 2 shows a similar trend as in the present investigation; Mach number was also shown to have an effect on the aerodynamic-center position. The difference in the results of the present and comparison configurations is attributed to the removal of the rear one-sixth portion of the body for the tests of reference 2.

The variation with Mach number of the static-longitudinal-stability derivative  $dC_M/d\alpha$ , for the body-plus-tail combination, is presented in figure 8. Two  $dC_M/d\alpha$  parameters are presented, one for the rolling condition and one corrected to the nonrolling condition. The faired value of  $dC_M/d\alpha$  for the model corrected to the nonrolling condition increases (decreasing stability) from approximately -5.75 at  $M = 0.7$  to -4.6 at  $M = 1.17$ . At higher Mach numbers the values of  $dC_M/d\alpha$  are doubtful because of the extrapolation of the rate-of-roll curve as was

previously discussed. The faired values of  $dC_M/d\alpha$  for the rolling condition increase (decreasing stability) from approximately -3.75 at  $M = 0.7$  to -3.0 at  $M = 1.15$ . Above this range the stability decreased rapidly to approximately -2.0 at  $M = 1.24$ . This rapid decrease in stability is indicative of a rapid buildup of roll.

The parameters for the body alone previously discussed ( $C_{NB}$  and aerodynamic-center location) indicate the body alone is unstable but becomes less unstable with increase in  $C_{NB}$  and  $M$ . The stability parameter for the complete model  $dC_M/d\alpha$  shows a decrease in stability with increase in  $C_{NB}$  and Mach number. It is assumed that the rate of roll above  $M = 1.26$  was of a magnitude that its destabilizing effect coupled with the destabilizing effects of increasing  $M$  produced an unstable condition and subsequent tumble of the model.

#### CONCLUDING REMARKS

The longitudinal stability and drag characteristics of a fin-stabilized body of revolution with a fineness ratio of 12 at low angles of attack have been investigated through the transonic speed range by the free-fall method.

The results showed that the aerodynamic center moved rearward from 55 percent body length ahead of the nose at a Mach number of 0.87 and a body normal-force coefficient of 0.11 to 15 percent ahead of the nose at a Mach number of 1.26 and a body normal-force coefficient of 0.24. The theory of NACA RM A9126 predicts approximately 60 percent of this shift in aerodynamic center with the increase in body normal-force coefficient. The difference in the investigation results and theory is assumed to be attributable to the effects of the increase in Mach number which accompanied the increase in normal-force coefficients. The same trend was indicated in the investigation of a similar model reported in NACA RM L52D21a.

The stability of the body-plus-tail combination decreased with increase in Mach number; the stability was further decreased by a buildup in roll velocity which ultimately produced an unstable configuration.

The longitudinal-force measurements agree favorably with the results of a similar body investigated at zero lift in the subsonic range of

speeds; however, in the supersonic range of speeds, the measurements were 20 percent less than the zero-lift drag of the similar configuration.

Langley Aeronautical Laboratory,  
National Advisory Committee for Aeronautics,  
Langley Field, Va., May 3, 1954.

#### REFERENCES

1. Allen, H. Julian: Estimation of the Forces and Moments Acting on Inclined Bodies of Revolution of High Fineness Ratio. NACA RM A9I26, 1949.
2. Estabrooks, Bruce B.: An Analysis of the Pressure Distribution Measured on a Body of Revolution at Transonic Speeds in the Slotted Test Section of the Langley 8-Foot Transonic Tunnel. NACA RM L52D21a, 1952.
3. Thompson, Jim Rogers: Measurements of the Drag and Pressure Distribution of a Body of Revolution Throughout Transition From Subsonic to Supersonic Speeds. NACA RM L9J27, 1950.
4. Phillips, William H.: Effect of Steady Rolling on Longitudinal and Directional Stability. NACA TN 1627, 1948.

TABLE I.- BODY COORDINATES

[All dimensions are in inches]

x	y	x	y
0	0	48.00	4.876
.60	.277	54.00	4.971
.90	.358	60.00	5.000
1.50	.514	66.00	4.955
3.00	.866	72.00	4.828
6.00	1.446	78.00	4.650
9.00	1.936	84.00	4.274
12.00	2.365	90.00	3.754
18.00	3.112	96.00	3.031
24.00	3.708	102.00	2.222
30.00	4.158	108.00	1.350
36.00	4.489	114.00	.526
42.00	4.719	120.00	.000

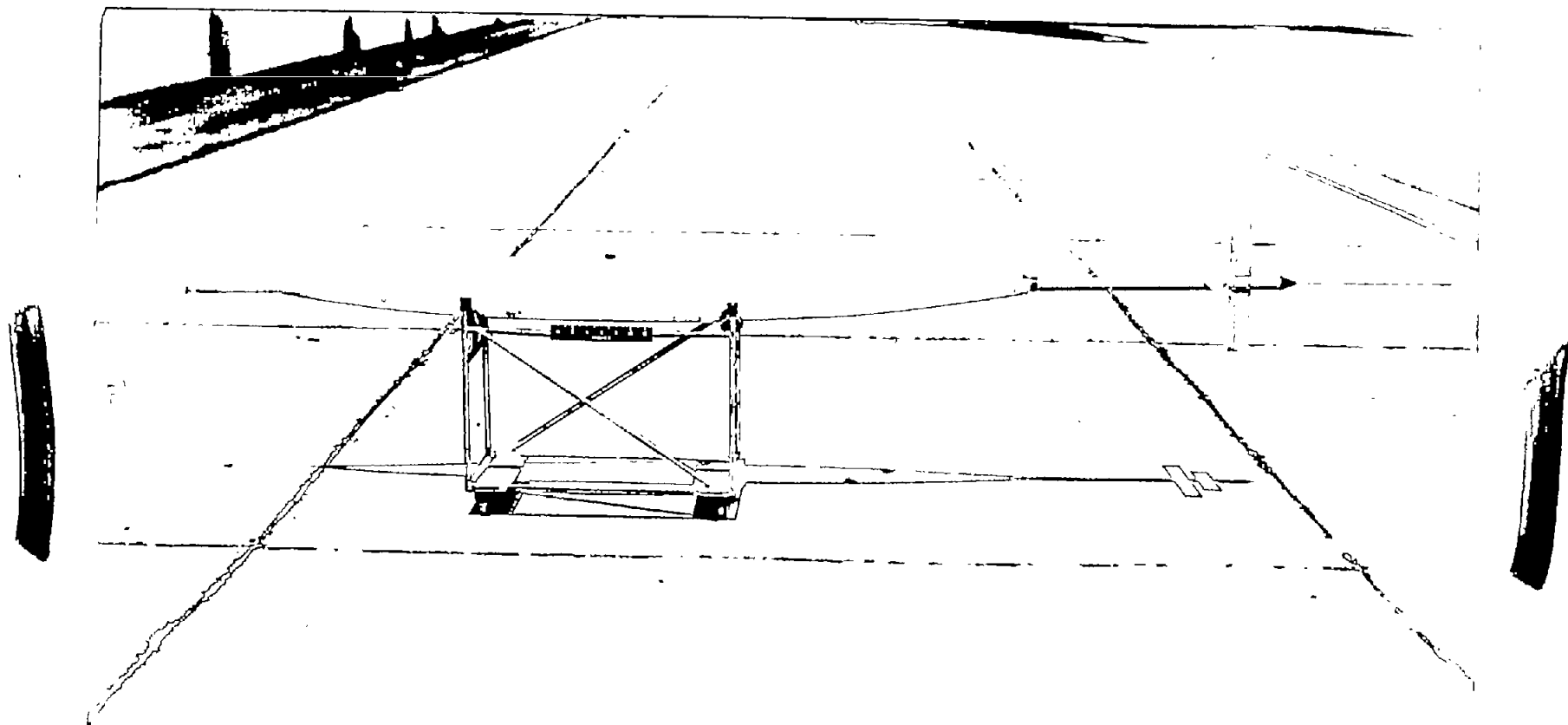


Figure 1.- Side view of model.

L-76441

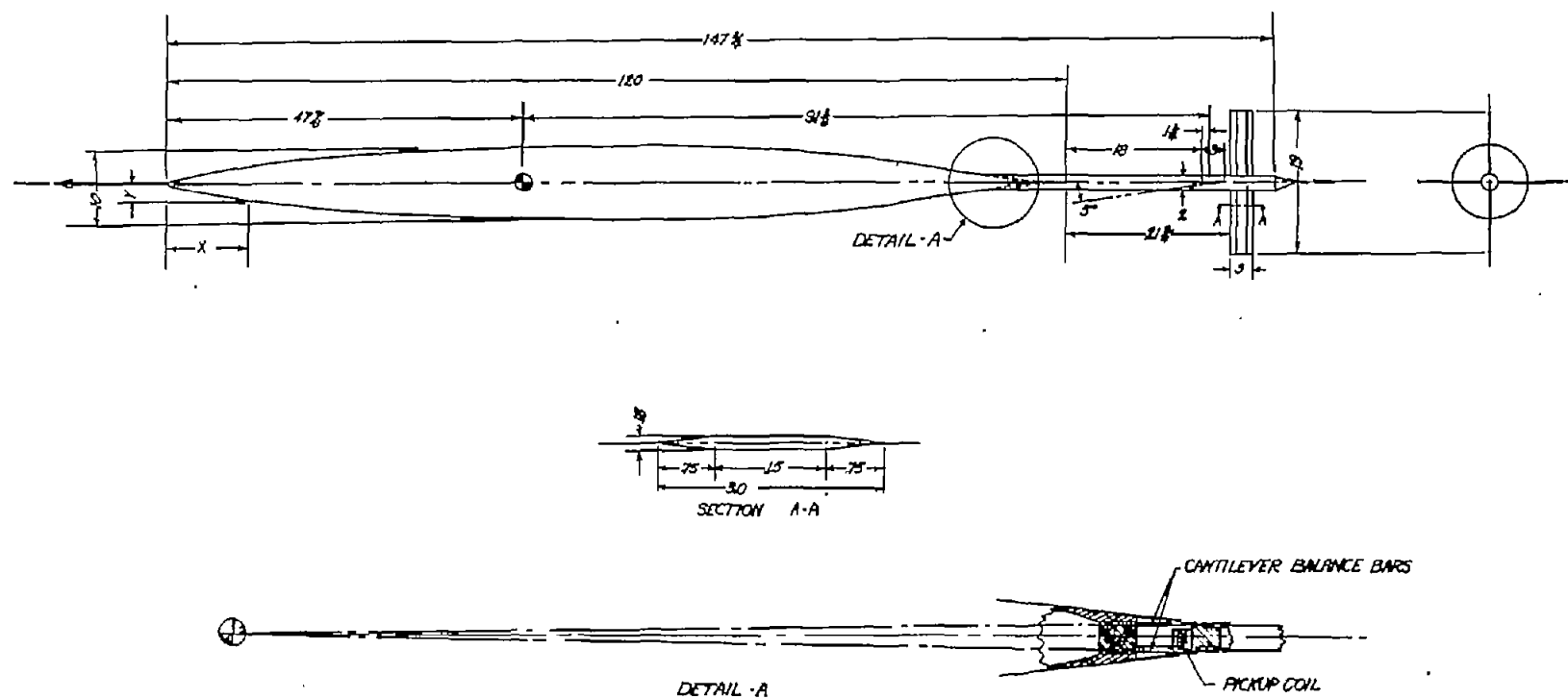
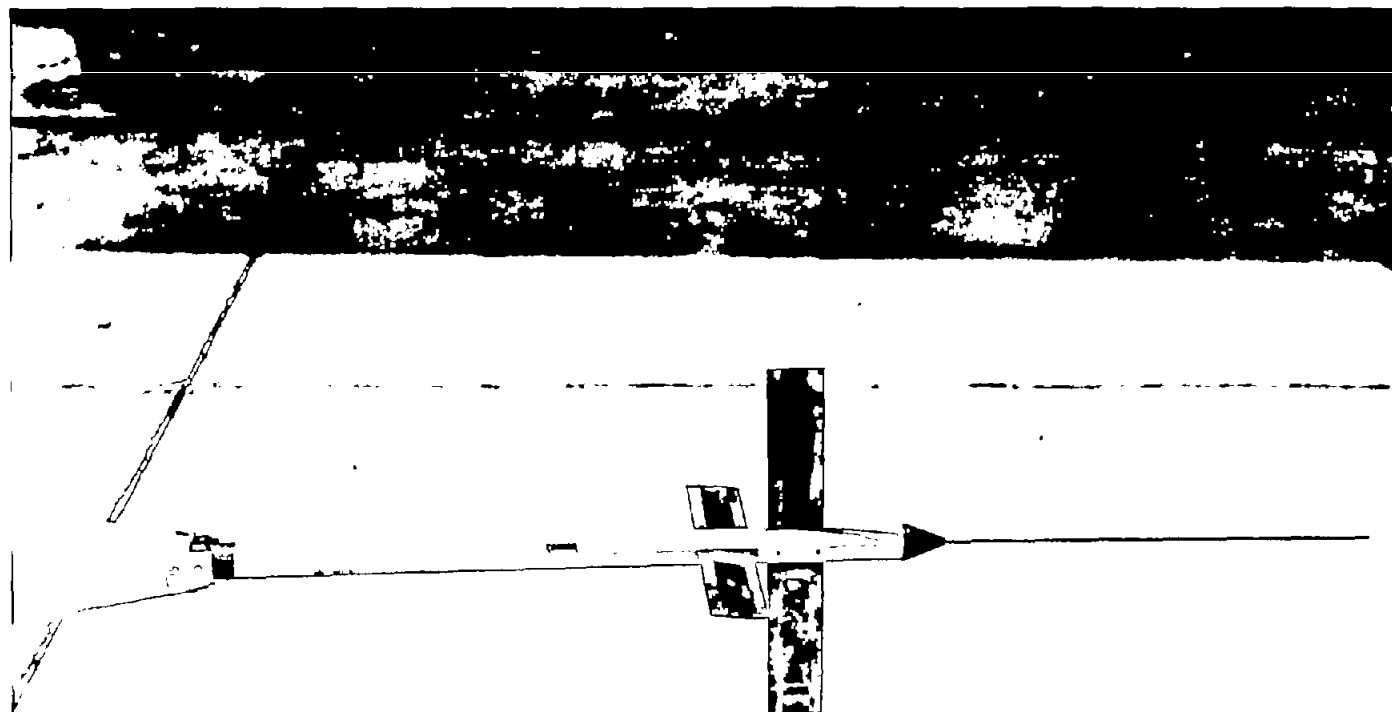


Figure 2.- Drawing of model. All dimensions are in inches.



L-76442

Figure 3.- View showing details of stabilizing fins, boom, and telemeter antenna.

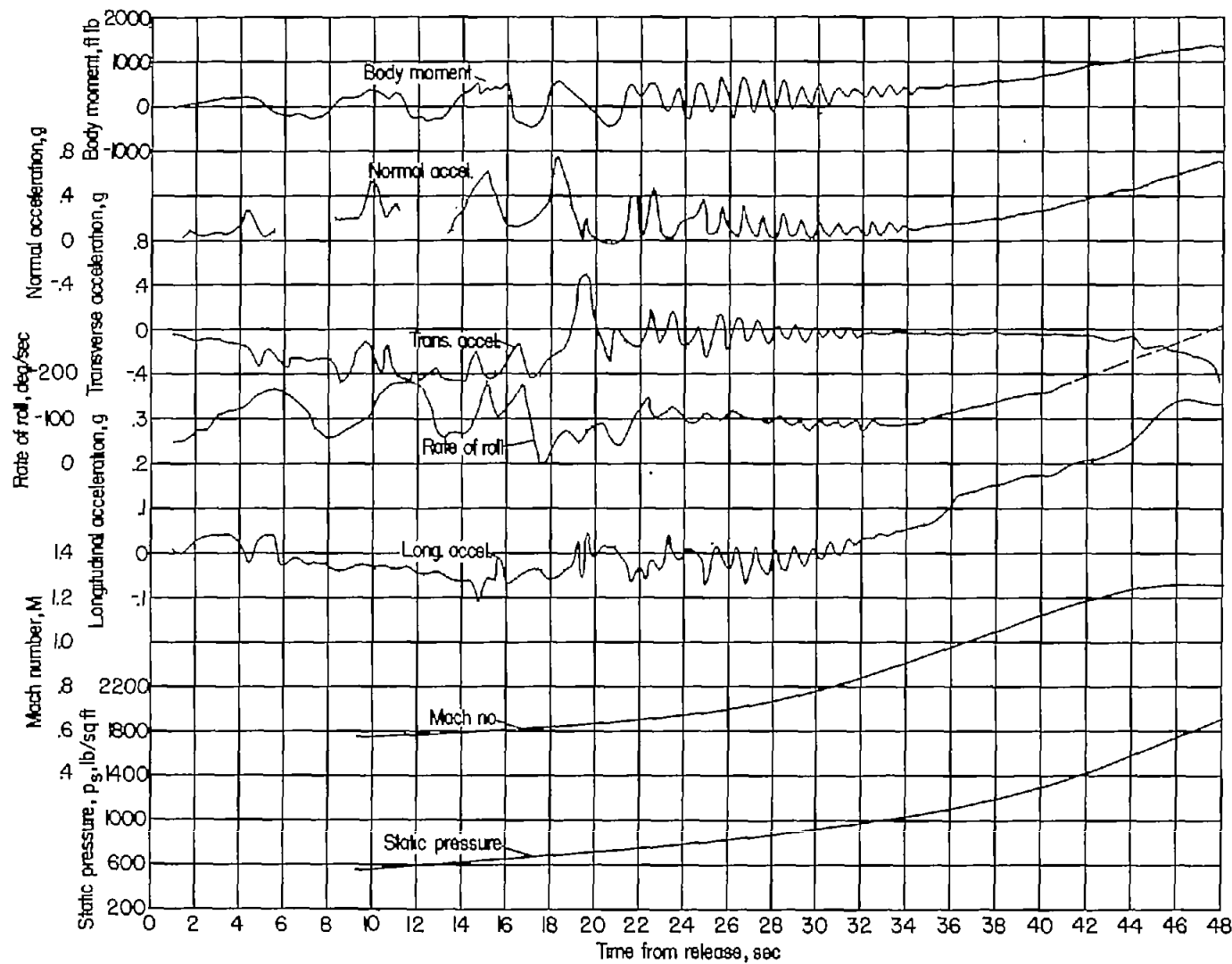


Figure 4.- Time history of free fall of model.



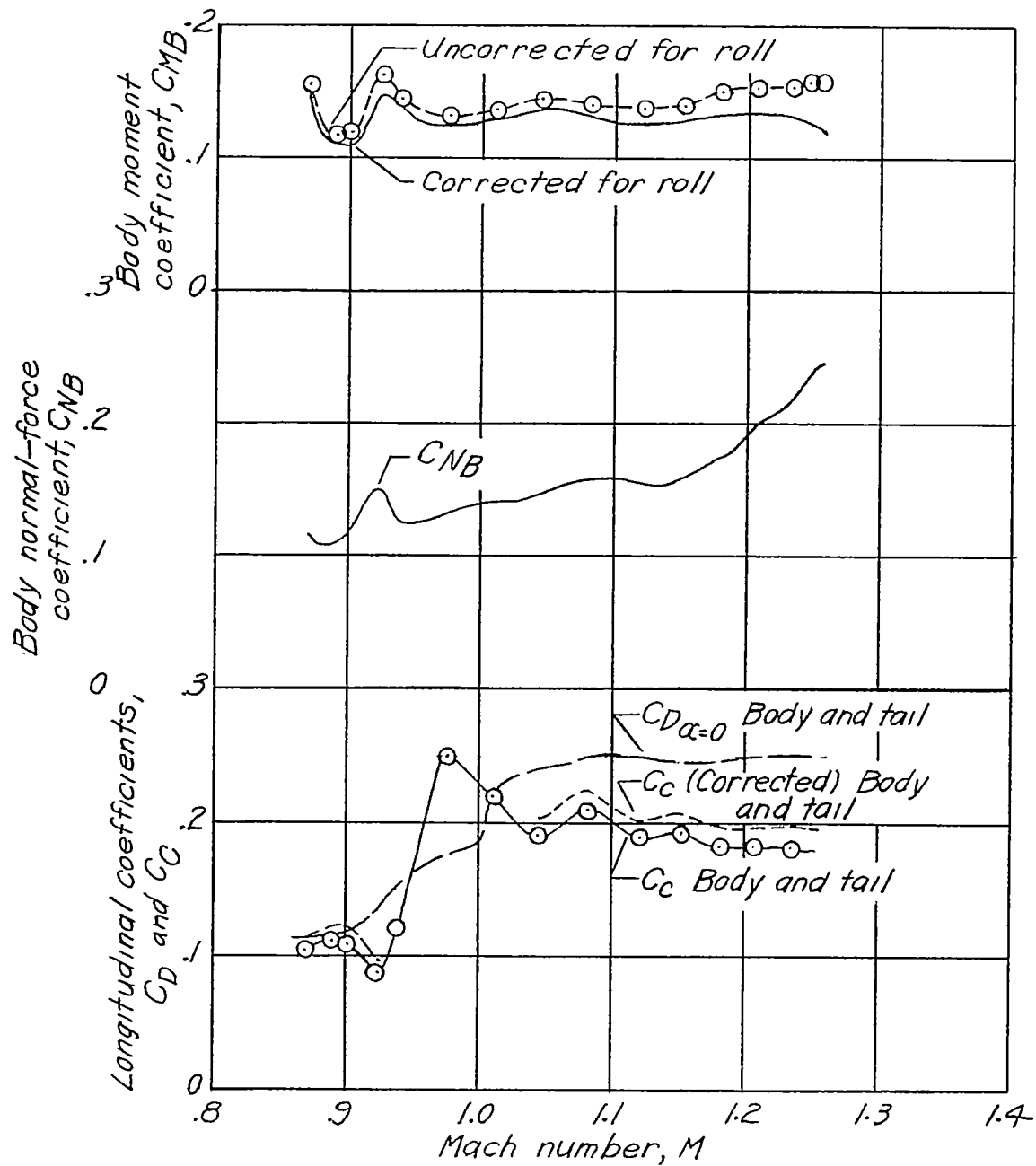


Figure 5.- Variation of body normal-force coefficient, body-plus-tail-combination chord-force coefficient, drag coefficient (zero lift), and body moment coefficient (rolling and nonrolling conditions) as a function of Mach number.

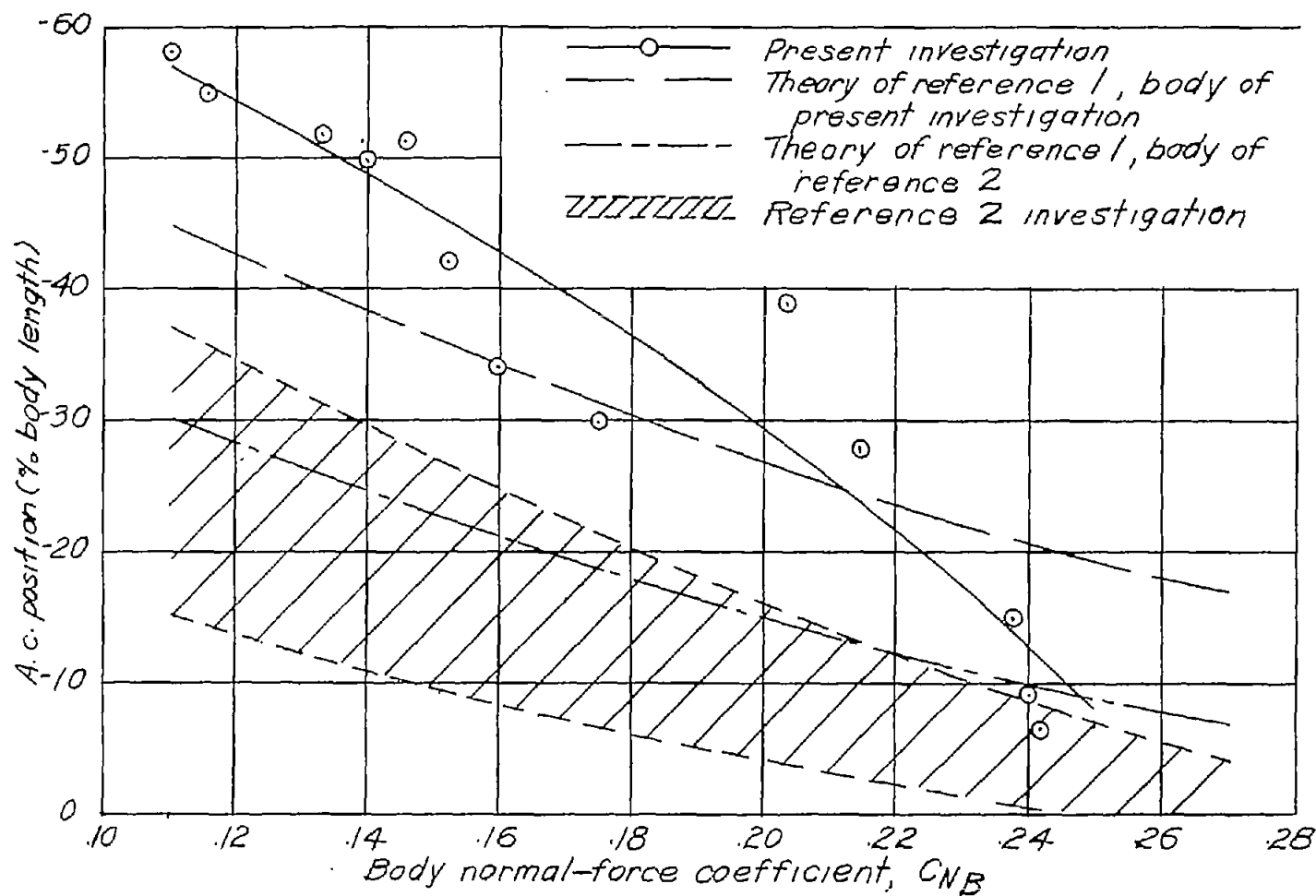


Figure 6.- Aerodynamic-center-position change as a function of body normal-force coefficient of body investigated, a similar body of reference 2, and theoretical change in aerodynamic center of both bodies as calculated by method of reference 1.

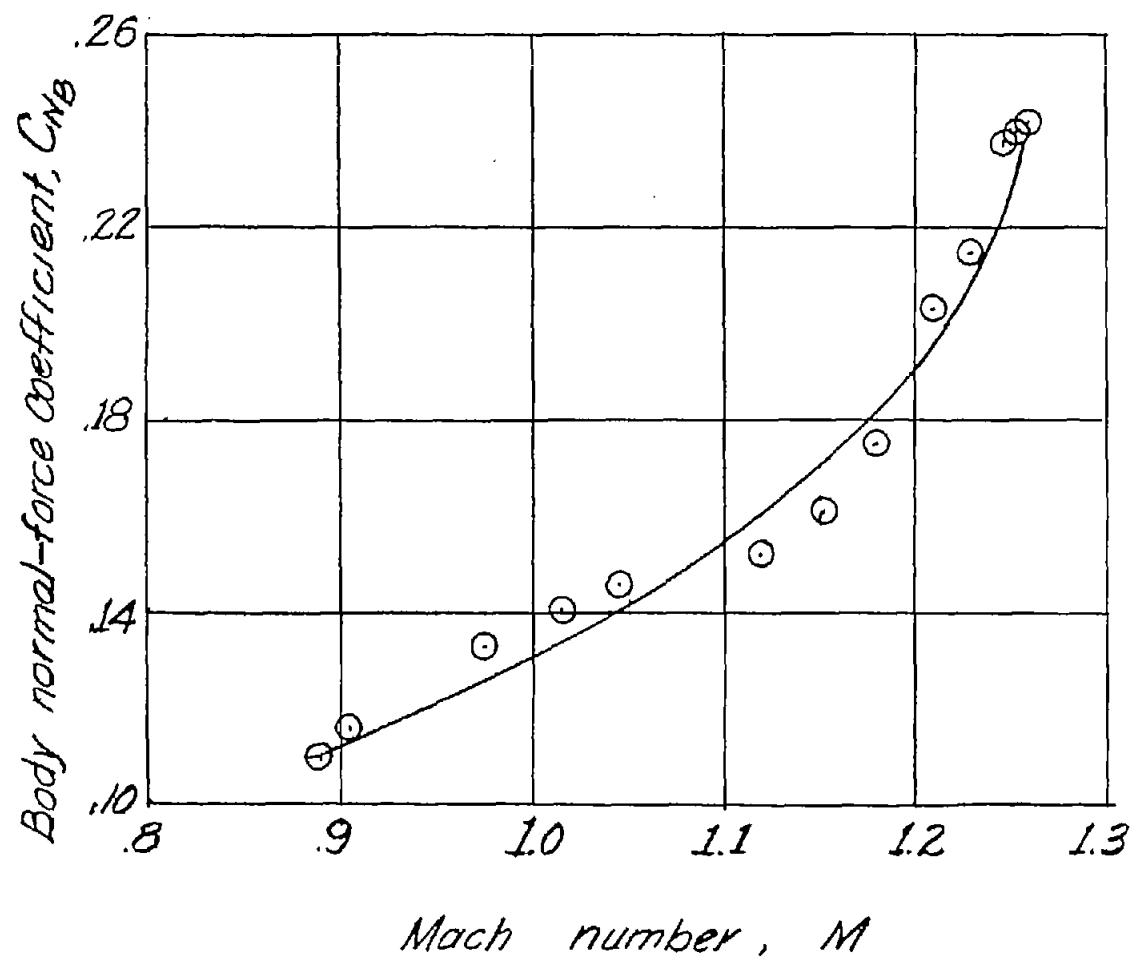


Figure 7.- Variation of body normal-force coefficient against Mach number for body of model investigated.

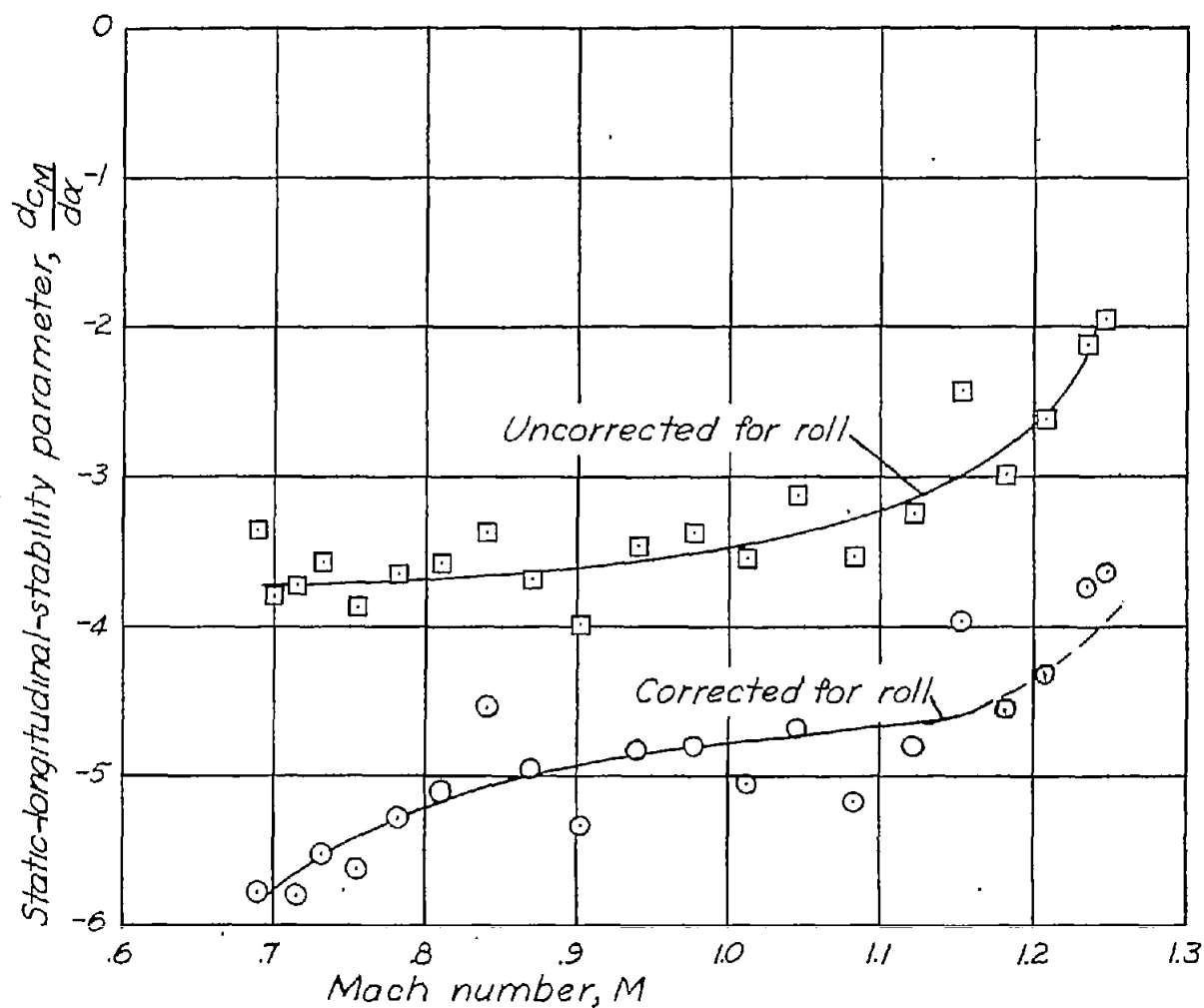


Figure 8.- Static-longitudinal-stability parameter  $\frac{dC_M}{d\alpha}$  as a function of Mach number for body and tail combination in rolling and nonrolling conditions.